

Table 1. Angular positions (2θ) of the crystalline peaks observed in the diffraction curve of Cellulose I

| Miller index (hkl) | 110 | 101 | $10\bar{1}$ | 021, 120, 200 | 002 | 122, 130, 131 | 103, 040 | 113, 320 | 004, 104, 332 |
|-----------------------------|-------|-------|-------------|---------------|-------|---------------|--------------|--------------|---------------------|
| Peak position (2θ) | 13.86 | 14.74 | 16.58 | 20.60, 21.83 | 22.67 | 29.69, 29.97 | 34.79, 34.85 | 35.90, 37.45 | 46.29, 46.33, 46.64 |

In this way the variables of incomparable quantities can be transformed into the same statistical measure. Thanks to such a transformation we can compare the changeability of these quantities.

The results presented in Figs. 2 and 3 indicate that the first six algorithms (from 1 to 6) generally met all requirements. Their effectiveness in determination of a good theoretical model of the experimental curve is comparable.

As one can see in Fig. 2, the informational criteria, *i.e.*, integral index S_y , normalized S_R index, standard error of estimation are the lowest for these algorithms, testifying that the theoretical and experimental curves are well fitted. In Fig. 3 we see that the Wald-Wolfowitz test, Wilcoxon test and series length test confirm the randomness of residuals for the algorithms 1–6. Moreover, the tests of normality (Chi-squared and Kolmogorov-Smirnov tests) prove that the distribution of residuals is normal and the test of symmetry shows that the distribution of residuals is symmetrical. Simultaneously, Fig. 2 shows that the worst quality of fitting (the highest information criteria S_y, S_R, S_e) are obtained for the algorithm 8. Also the results of statistical tests for this algorithms (see Fig. 3) are much worse than for the remaining ones (residuals are not random, their distribution is not normal, *etc.*). Besides, much lower quality of fitting is observed for the algorithm 7 (Fig. 2). Concluding, the algorithms 7 and 8 should not be employed in decomposition of the WAXD curves of Cellulose I. On the other hand, a detailed analysis of the plots in Figs. 2 and 3 leads to the conclusion that the best results are obtained using the algorithm 3.

Figure 4 presents ten theoretical curves and their amorphous components, obtained by means of PSO optimization procedure equipped with the algorithm 3 (10 independent runs of the procedure). As one can see, the curves are superimposed on one another to such a degree that practically they are undistinguishable. Also the differences between the amorphous components are very small. This result confirms that the algorithm 3 leads to nearly univocal solutions.

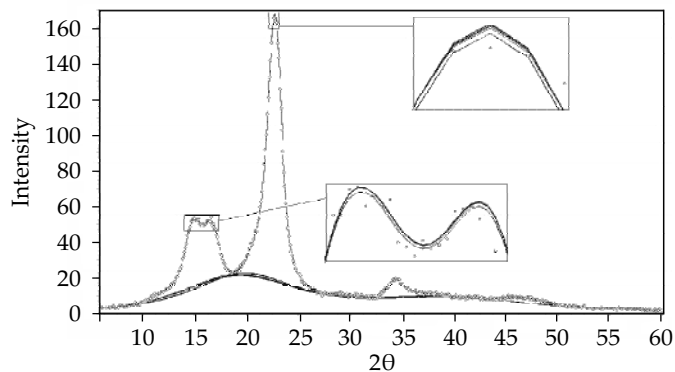


Fig. 4. Experimental (points) and ten theoretical (solid lines) WAXD curves of Cellulose I with their amorphous components obtained by means of a PSO optimization procedure equipped with the algorithm 3; the inserts show two magnified fragments of the plot

Cellulose II and PET

The WAXD curves of Cellulose II and PET with the best fitted theoretical curves are shown in Figs. 5–10. The curve of Cellulose II (Fig. 5) contains eleven crystalline peaks and two amorphous maxima. In the curve of PET (Fig. 8) there are thirteen crystalline peaks and two amorphous maxima. The positions of crystalline peaks of Cellulose II and PET determined by the optimization procedure are given in Table 2 and Table 3 respectively.

Comparing them with Figs. 2 and 3 we see that for all three polymers, the results are very similar. So, based on this fact we can formulate the same conclusion: the first six algorithms give reliable theoretical curves, well fitted to the experimental ones and the requirements related to the residuals are fulfilled for these curves. Similarly as for Cellulose I, the algorithms 7 and 8 give worse quality of fitting and worse results of statistical tests. For this reason they should be rejected. A careful analysis of Figs. 5–10 shows that in the case of Cellulose II and PET the best results are obtained with the algorithms 1 and 2.

Table 2. Angular positions (2θ) of the crystalline peaks observed in the diffraction curve of Cellulose II

| Miller index (hkl) | 101 | $\bar{1}01$ | 021 | $\bar{1}11$ | 002 | 031 | 103 | 040, 311 | 310 | $10\bar{3}, 20\bar{2}, 20\bar{1}$ | $32\bar{1}$ |
|-----------------------------|-------|-------------|-------|-------------|-------|-------|-------|--------------|-------|-----------------------------------|-------------|
| Peak position (2θ) | 12.05 | 20.03 | 20.50 | 21.83 | 22.03 | 28.25 | 29.49 | 34.85, 34.80 | 38.59 | 40.98, 40.72 | 47.78 |

Table 3. Angular positions (2θ) of the crystalline peaks observed in the diffraction curve of PET

| Miller index (hkl) | $0\bar{1}1$ | 010 | $\bar{1}11$ | $\bar{1}10$ | 011 | $\bar{1}12$ | 100 | $\bar{1}03$ | $1\bar{1}1$ | 101 | $\bar{1}05$ | $20\bar{1}, \bar{1}30$ | 112 |
|-----------------------------|-------------|-------|-------------|-------------|-------|-------------|-------|-------------|-------------|-------|-------------|------------------------|-------|
| Peak position (2θ) | 16.45 | 17.45 | 21.30 | 22.57 | 23.37 | 24.63 | 25.60 | 26.45 | 27.85 | 32.65 | 42.60 | 47.13 | 53.38 |

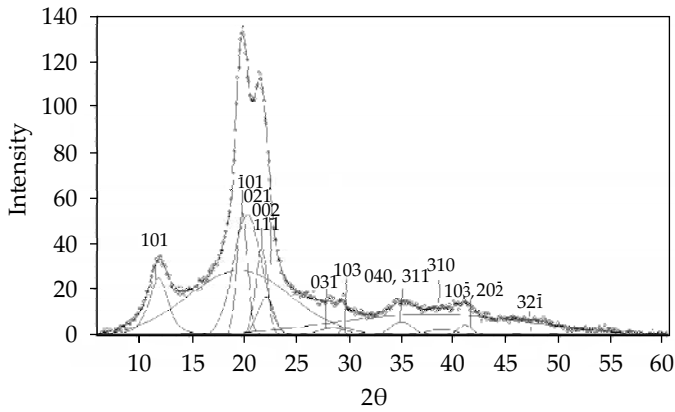


Fig. 5. WAXD curve of Cellulose II decomposed into crystalline peaks and amorphous component by means of PSO algorithm; experimental curve – points, the best fitted theoretical curve and its all elements (11 crystalline peaks and 2 amorphous maxima) – solid line

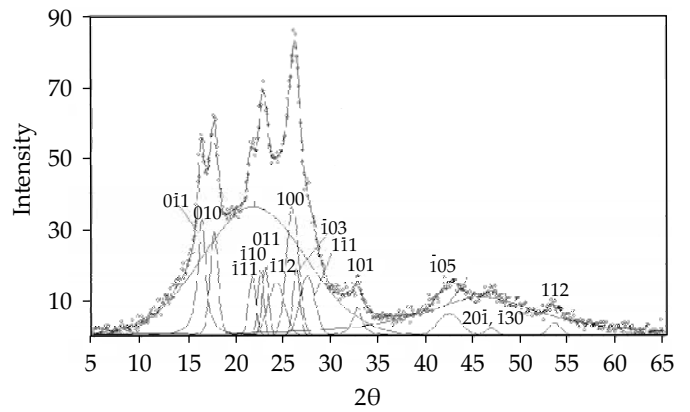


Fig. 8. WAXD curve of PET decomposed into crystalline peaks and amorphous component by means of PSO algorithm; experimental curve – points, the best fitted theoretical curve and its all elements (13 crystalline peaks and 2 amorphous maxima) – solid line

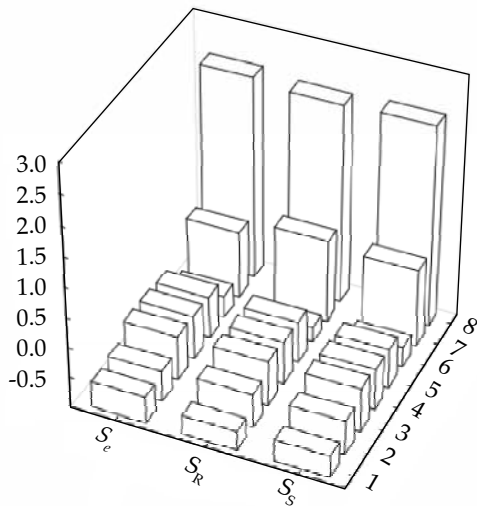


Fig. 6. A comparison of the information criteria obtained for the analyzed algorithms in the case of WAXD curve of Cellulose II; to present them in one plot the criteria were pre-standardized

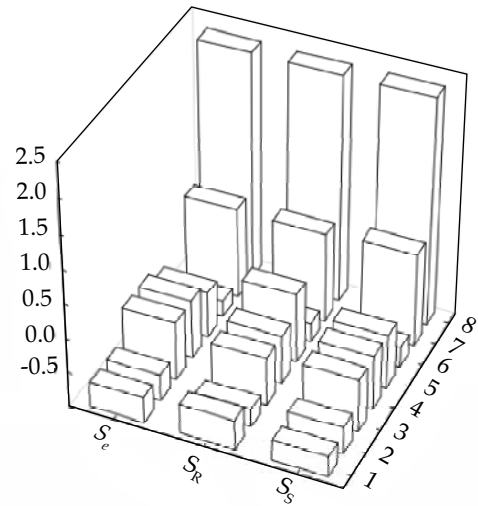


Fig. 9. A comparison of the information criteria obtained for the analyzed algorithms in the case of WAXD curve of PET; to present them in one plot the criteria were pre-standardized

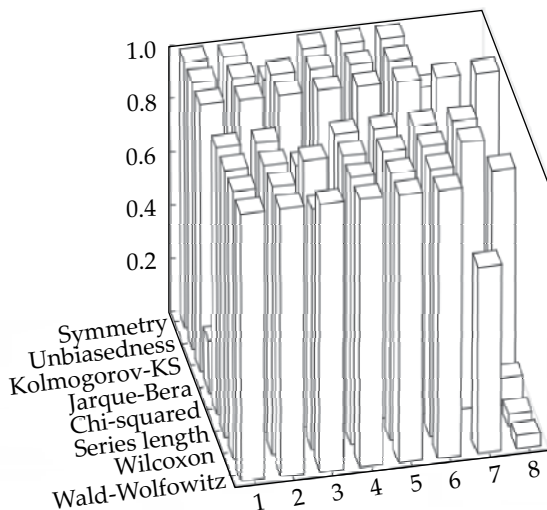


Fig. 7. The results of statistical test for the WAXD curve of Cellulose II

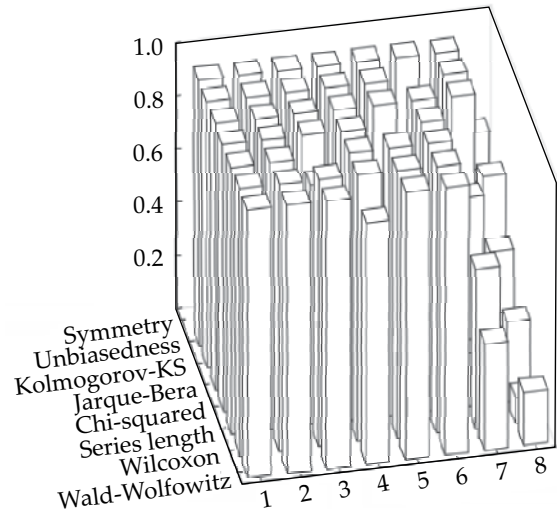


Fig. 10. The results of statistical test for the WAXD curve of PET

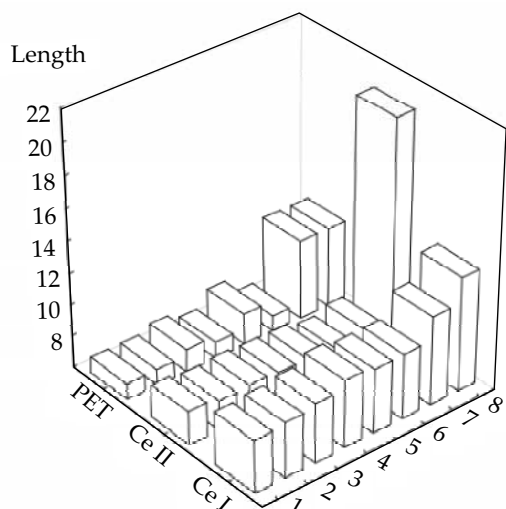


Fig. 11. The longest series of points in the WAXD curve for which the theoretical curve is not fitted to the experimental one

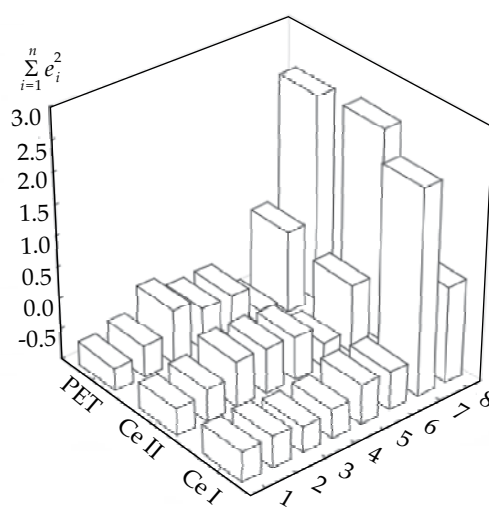


Fig. 12. Standardized values of the final sum of squared residuals obtained with tested algorithms

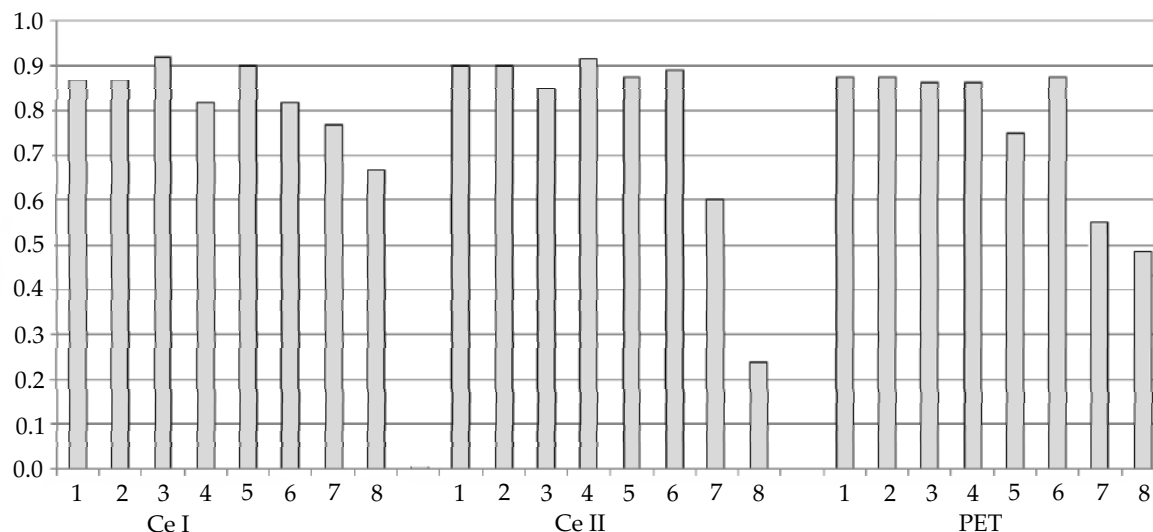


Fig. 13. The average value of all tests (8) achieved by a given algorithm (from 1 to 8) for investigated polymers

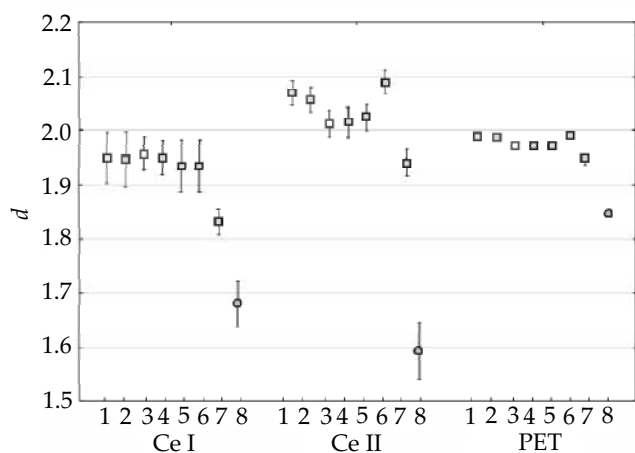


Fig. 14. Values of the Durbin-Watson d statistic achieved by a given algorithm (1–8) for investigated polymers

A comparison of the algorithms based on the results obtained for the WAXD curves of all investigated polymers

The Figs. 11–14 present a comparison of the averaged results of statistical tests achieved by the analyzed algorithms. For each WAXD curve the optimization procedure equipped with a given algorithm has been run for 10 times.

Obtained results show that for all investigated polymers the optimization procedures equipped with the algorithms 7 and 8 give models (theoretical curves) characterized by the lowest quality of fitting, the longest series of points at which the theoretical curve is not fitted to the experimental one, the worst value of the Durbin-Watson d statistic and the biggest values of the final sum of squared residuals. Furthermore, according to performed statistical tests, the requirements related to the residuals